fluids

MDPI

Article

Velocity Distribution in Channels with Submerged Vegetation

Aristotelis Mavrommatis and George Christodoulou *

Applied Hydraulics Laboratory, School of Civil Engineering, National Technical University of Athens, 5 Heroon Polytechniou, 15780 Zografou, Greece
* Correspondence: christod@hydro.ntua.gr

Abstract: An experimental study is presented for investigating the effect of vegetation element geometry on the velocity distribution within and above the canopy. Three types of artificial submerged vegetation elements with common parts and different foliage are used, with two density patterns each. Detailed velocity profiles are obtained and compared at nine locations in the vegetation array. The velocity distribution above the canopy is found to closely follow a logarithmic law and its parameters, namely the shear velocity u*, zero-plane displacement height d and roughness height z_0 are determined. These depend on the vegetation density and type of element, but also on the particular position in the array. A unified velocity distribution over the water column is found appropriate for the case of stems with no foliage and also for the cases of compound elements at certain positions in the vegetation array but not at those where locally minimum velocity values occur at the foliage level. Moreover, the logarithmic profile obtained for the upper layer is seen to also fit well the measured velocities to a certain extent below the top of the canopy.

Keywords: open channel flow; vegetation; velocity distribution; velocity profile

Citation: Mavrommatis, A.; Christodoulou, G. Velocity Distribution in Channels with Submerged Vegetation. *Fluids* **2022**, *7*, 290. https://doi.org/10.3390/fluids7090290

Academic Editors: Mehrdad Massoudi and Ashwin Vaidya

Received: 29 June 2022
Accepted: 29 August 2022
Published: 31 August 2022

1. Introduction

The presence of vegetation in channels, streams and riparian zones is highly important for environmental and ecological reasons but significantly affects the flow conditions. Vegetation stems and foliage offer increased resistance to the flow, leading to flow retardance, affecting the diffusion of nutrients and contaminants, promoting sedimentation and providing sheltered habitats to aquatic species. Early studies of flow in vegetated channels focused mainly on resistance characteristics, exploring modifications to the Manning formula or the determination of appropriate friction coefficients [1–3]. Velocity distribution has also received considerable attention, since it is related to the overall resistance, but also to local flow features, turbulence and shear stress distribution in the water column.

When vegetation (either rigid or flexible) is submerged, the top of the canopy clearly defines an interface between two layers, above and within the vegetation. Based on this concept, several researchers proposed two-layer models with empirical equations describing the velocity distribution, and they evaluated the relevant parameters by comparing with experimental results. For example, Klopstra et al. [4] developed an analytical, physically based model of the vertical flow velocity profile, applying different turbulence models for the vegetation layer and the surface layer. Huthoff et al. [5] described flow above and through the vegetation layer separately and proposed a model for the quick evaluation of a river's hydraulic response in cases of vegetated floodplains. Righetti and Armanini [6] conducted experiments in a channel with sparsely arranged bushes simulated by spheres and proposed a two-layer model consisting of a logarithmic profile in the upper non-vegetated layer and a power-law profile in the vegetated layer. Huai et al. [7] used the predicted deflection height of flexible vegetation determined by the large-deflection cantilever beam theory, separated the flow into a bottom vegetated layer and an upper free water layer and formulated momentum equations for each layer.

On the other hand, a three-layer approach has been adopted by many other researchers. According to Shi and Hughes [8], the velocity profile can be roughly divided into three hydrodynamic zones: one within the canopy, one above the canopy and an intermediate transitional one. In fact, at the interface between the vegetated layer and the upper unobstructed layer, a shear layer develops, as discussed by Nepf [9] as well as Ghisalberti and Nepf [10]. Furthermore, Nepf and Vivoni [11] identified two regions within the vegetation, i.e., the upper part of canopy where vertical turbulent exchange with the free unobstructed zone is dynamically significant to the momentum balance, whereas in the lower part of canopy, longitudinal advection is predominant, and the momentum equilibrium is a balance of vegetative drag and the pressure gradient. Carollo et al. [12] proposed a single equation for the entire water column, featuring an inflection point at the top of the canopy and tending asymptotically to the maximum and minimum velocity at the free surface and the bottom, respectively. Ghisalberti and Nepf [10] also proposed a unified velocity profile but with the inflection point lower than the top of the canopy by a quantity related to the momentum thickness of the mixing layer. It may be noted that the existence of an inflection point is not universally observed, e.g., for low vegetation densities (Nepf [9]). Huai et al. [13] showed that the velocity profile consists of three hydrodynamic regimes adopting different methods for each layer to describe the vertical velocity distribution. Chen et al. [14] studied several patterns of flexible vegetation bundles and proposed a three-layer model, with different logarithmic equations expressing the velocity distribution at each layer depending also on different measurement positions. Li et al. [15] used new mathematical expressions to express variations in the velocity profile, in the Manning coefficient and in the flow discharge ratio for various vegetation densities.

Despite the conceptual differences in the approach of previous works, there is predominant agreement that the velocity distribution above the vegetation canopy closely follows a logarithmic law similar to the well-known von Karman law of the wall in a boundary layer. Variants of this law applicable to vegetated channels have been proposed by Stephan and Gutknecht [16], Liu et al. [17] and others, but the simplest and most commonly used form is [4,8,10]:

$$u/u^* = 1/k \ln((z - d)/z_0) \quad (1)$$

where u = the local velocity at height z, u* = the shear velocity, k = 0.4 von Karman constant, d = the zero plane displacement height and z_0 = the roughness height. Equation (1) is also often employed for the velocity profile of air flow above terrestrial canopies, e.g., as described by Raupach [18,19]. Several researchers have proposed ways of estimating the parameters of Equation (1), namely u*, d and z_0, depending on some canopy characteristics based on experimental data. Below the top of vegetation, the flow is highly heterogeneous and seems to strongly depend on the density, shape and flexibility of vegetation elements, relative submergence, etc. For vertically uniform vegetation, the velocity usually decreases gradually towards the bottom, whereas in the case of plants consisting of stem and leaf sections, the distribution may have a minimum at about the level of foliage [14]. Therefore, proposing a unified velocity distribution model is more difficult.

Most of the aforementioned developments are based on experimental measurements. However, little information exists about the spatial variability of the flow features within the vegetation and the influence of the type/geometry of vegetation elements. This is because most previous studies are based either on a single type of element or have reported results as spatial averages or only on the channel axis. For example, Fairbanks [20] and Liu et al. [17] reported detailed velocity measurements at six positions in an array of cylindrical elements on a parallel and a staggered pattern. Dunn et al. [21] presented average profiles for rigid and flexible cylinders in a staggered pattern. Righetti and Armanini [6] also reported average profiles for an array of artificial bushes, whereas Shi et al. [8], Chen et al. [14] and Li et al. [15] used real or artificial vegetation and presented results only at locations along the channel axis. However, a recent study by the authors [22] provides evidence that the velocity distribution may vary depending on the type of element and also on the

location within the vegetation array. Such details may be important with respect to the local transport processes and ecological habitat and therefore deserve further investigation.

Considering the above, the objective of the present paper is to further explore the velocity distribution in channels with submerged vegetation by quantitatively studying the variations in relevant parameters for different geometries or densities of vegetation elements as well as the spatial variation of the profiles within and above the vegetation, depending on location in the vegetation array.

2. Materials and Methods

Experiments were carried out in a laboratory channel with glass walls, 16 m long and 0.50 m wide, with a slope of 0.001. Six different experimental conditions were examined under a constant flow rate and depth in the measurement area, attained by an adjustable sluice gate at the end of the channel. The flow rate was Q = 41 L/s, recorded by means of a Venturi meter and a differential manometer installed in the laboratory supply line with an accuracy of $\pm$ 0.5 L/s. The flow depth was H = 25 cm, measured by a point gauge along the channel axis with an accuracy of $\pm$ 0.2 cm. In all cases, the flow in the channel was turbulent with a Reynolds number, based on flow depth, of Re = 82,000. A general view of the experimental channel with vegetation is shown in the photo of Figure 1. Three types of vegetation elements were tested, simulating submerged small plants, as shown in Figure 2: (a) rigid rods without foliage of diameter d = 0.5 cm and height h = 4 cm; (b) rigid rods of d = 0.8 cm and h = 5 cm with dense (rigid) foliage, simulated by plastic spheres 3.0 cm in diameter fixed on top of the rods; and (c) rigid rods of d = 0.8 cm and h = 5 cm with sparse semi-flexible foliage, simulated by 2–2.5 cm-long plastic needles arranged symmetrically on top of the same rods. The elements were placed on a false perforated bottom at a parallel and a staggered pattern, with respective plan densities of 100 and 200 stems/m^2, as depicted in Figure 3a,b. These two patterns, with various densities, are the simplest and most commonly used in previous works [2,6,13,14,20,21]. Being horizontally uniform, they are suitable for revealing the degree of the variability of flow features due to the geometry of the elements or the location. The frontal density of vegetation, λ, defined as the ratio of the elements' frontal area per unit channel bottom area, ranged between 0.020 and 0.222. The submergence ratio H/h was always larger than 2, ensuring no influence of the free surface [11]. The stem Reynolds number, based on the stem diameter, was about 1640 for the simple rods and 2620 for the compound elements, i.e., well above the critical value of 200 [11], ensuring fully turbulent wakes within the vegetation array. A baseline experiment with no vegetation for the same flow rate and depth was also conducted. Table 1 lists the main characteristics of the experimental sets.

Velocity measurements were obtained by means of a 3-D Acoustic Doppler Velocimeter (ADV Lab Ver. 2.7 Probe N0187 Nortec AS, Sandvika, Norway) on vertical lines at selected locations within the vegetation array (denoted as A, B, C, D, E, F, G, H, I), shown in Figure 3c. ADV instruments have been widely used in previous studies [11–15,21] for point measurements in vegetated flows. The duration of each measurement was 2 min, the sampling frequency was 25 Hz and the accuracy was $\pm$ 0.01 cm/s. Velocities were recorded at several points up to a height of 19 cm, as the ADV cannot operate properly close to the free surface. Locations A and C were accessible only in Exp1 and Exp2, whereas location H was only for the parallel vegetation pattern (Exp1, Exp3 and Exp5).

Figure 1. General view of the experimental setup.

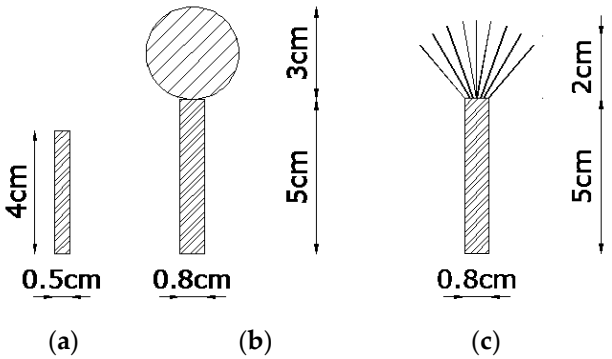

Figure 2. Vegetation elements: (**a**) simple rod, (**b**) compound rigid and (**c**) compound semi-flexible.

Table 1. Sets of experiments.

Experiment	Vegetation Pattern	Vegetation Type	Vegetation Density (stems/m^2)	Element Height h (cm)	Frontal Density λ	Submergence Ratio H/h
Exp0	no vegetation					
Exp1	parallel	simple rigid	100	4	0.020	6.250
Exp2	staggered	simple rigid	200	4	0.040	6.250
Exp3	parallel	compound semi-flexible	100	7	0.071	3.571
Exp4	staggered	compound semi-flexible	200	7	0.142	3.571
Exp5	parallel	compound rigid	100	8	0.111	3.125
Exp6	staggered	compound rigid	200	8	0.222	3.125

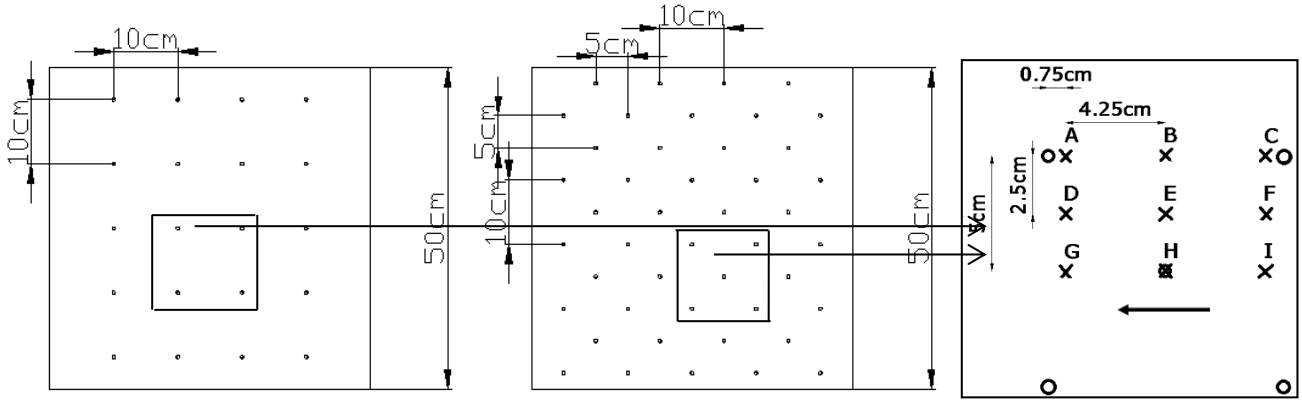

(**a**) (**b**) (**c**)

Figure 3. Vegetation patterns (a) parallel at 100 stems/m^2 and (**b**) staggered at 200 stems/m^2; (**c**) Measurement locations (x) within the vegetation array (arrow denotes the flow direction).

3. Results and Discussion

3.1. General Observations

Figure 4 shows a comprehensive comparison of normalized velocity profiles (u/u_h vs. z/h) at locations B, C, D, E, H and I for all experimental sets, where u_h denotes the velocity at the element top ($z = h$) at the respective location. Profiles at A, F and G (not shown) are very similar to those at C, D and I, respectively. Normalization in terms of u_h was chosen following previous works (e.g., as in [20]), so as to clearly elucidate the form of the profile above and below the top of canopy. For Exp0, a conventional value of h = 4 cm was considered, as in the case of simple rods (Exp1 and Exp2).

Considerable differences were observed between different experimental sets and also between measurement locations in each experimental set. In most cases, a significant reduction in velocity (relative to the no-vegetation case) occurred in the vegetation layer. This was more pronounced in presence of the compound elements compared to the simple stems and for the denser pattern for a given type of element. In the experiments with compound elements, the minimum velocity was recorded at the level of the upper (more bulky) part of the element and in certain locations (D, F) tending to zero. It is noticeable that these locations were between the elements' alignment, indicating the strong lateral interaction of wakes produced by the foliated vegetation elements. However, the type of foliage appeared to be of secondary importance. In the experiments with simple rods, the minimum velocities were observed close to the bottom and, as expected, at location C (and A), which were very close to the elements. Moreover, for the low density of rods (Exp1), the distribution far from the elements (e.g., at D, E, G, H) was very close to the no-vegetation case (Exp0).

3.2. Velocity Distribution above the Vegetation

Raupach [19] studied the application of Equation (1) for the velocity distribution above terrestrial canopies, considering the height h of vegetation elements and the frontal density λ as independent variables. He found that the ratio of the shear velocity u* to the velocity u_h at the top of the canopy may be expressed as:

$$\gamma = u_h/u^* = \exp(c\lambda\gamma/2)(C_S + C_R\lambda)^{-0.5} \quad (2)$$

where c, C_S and C_R are numerical constants with proposed values c = 0.5, C_S = 0.003 and C_R = 0.3. Equation (2) requires an iterative solution to obtain u_h/u^*. Furthermore,

he proposed the following equations for the zero-plane displacement height d and the roughness height z_0:

$$z_0/h = (1 - d/h)\exp(-ku_h/u^* - \Psi_h) \quad (3)$$

$$1 - d/h = [1 - \exp(-(c_{d1}2\lambda)^{0.5})]/(c_{d1}2\lambda)^{0.5} \quad (4)$$

where k = 0.4 is the von Karman constant, and Ψ_h and c_{d1} are numerical constants, with proposed values $\Psi_h = 0.193$ and $c_{d1} = 7.5$.

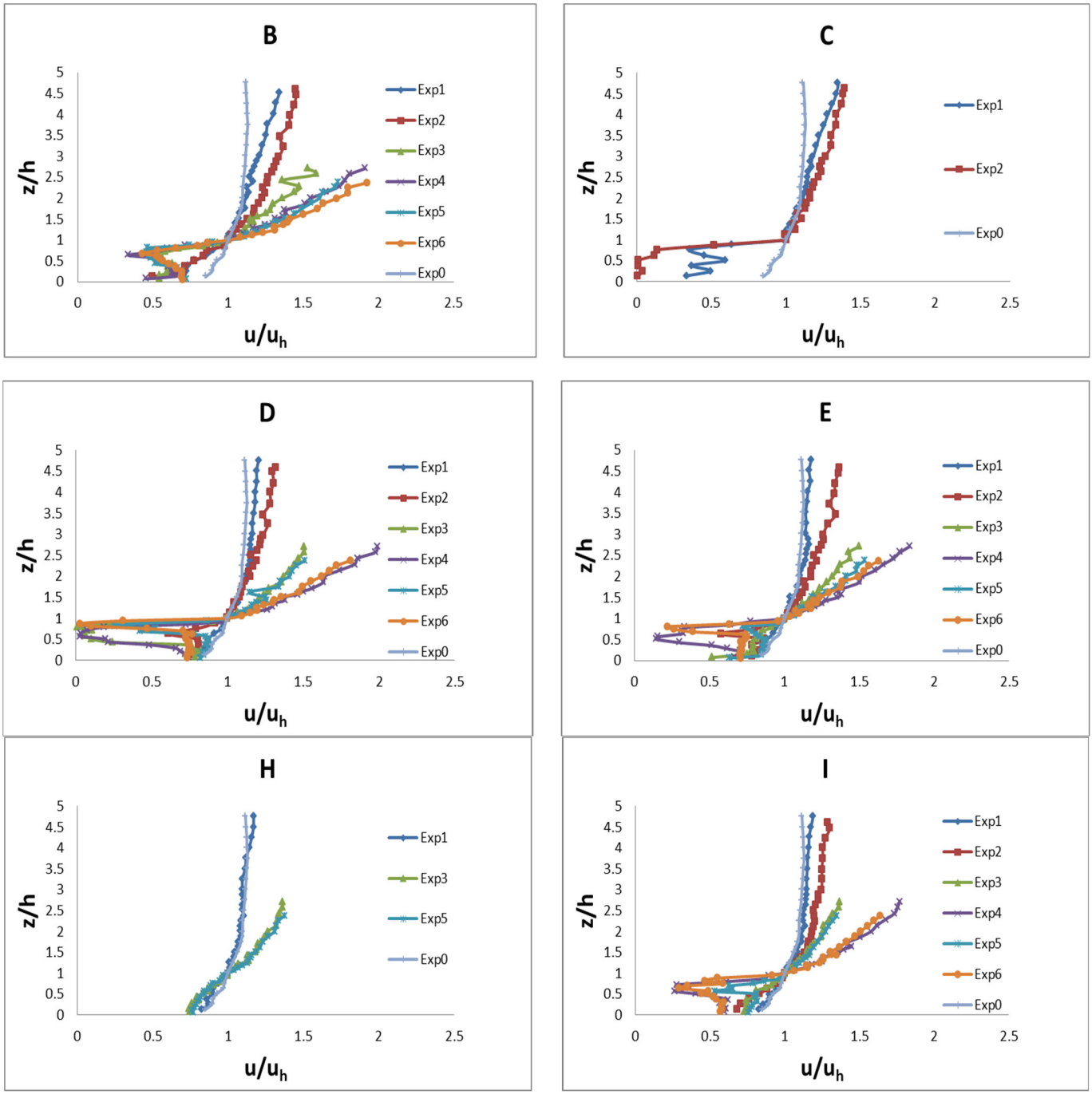

Figure 4. Normalized velocity profiles at locations: B, C, D, E, H and I.

The approach of Raupach was implemented in the context of the present study as follows: First, for each set of experiments, the values of u_h/u^*, d and z_0 were evaluated

based on Equations (2)–(4) according to the respective value of λ shown in Table 1. Then, the logarithmic law (Equation (1)) was fitted to the velocity measurements for z > h at each measurement position. Thus, the local value of u* was obtained as the slope of the fitting line in a semi-log plot. In general, a very good fit was observed, thus confirming the validity of Equation (1). In fact, in several cases, the applicability of Equation (1) appeared to extend below the top of the canopy. As an example, the plots for location B for all experiments are shown in Figure 5.

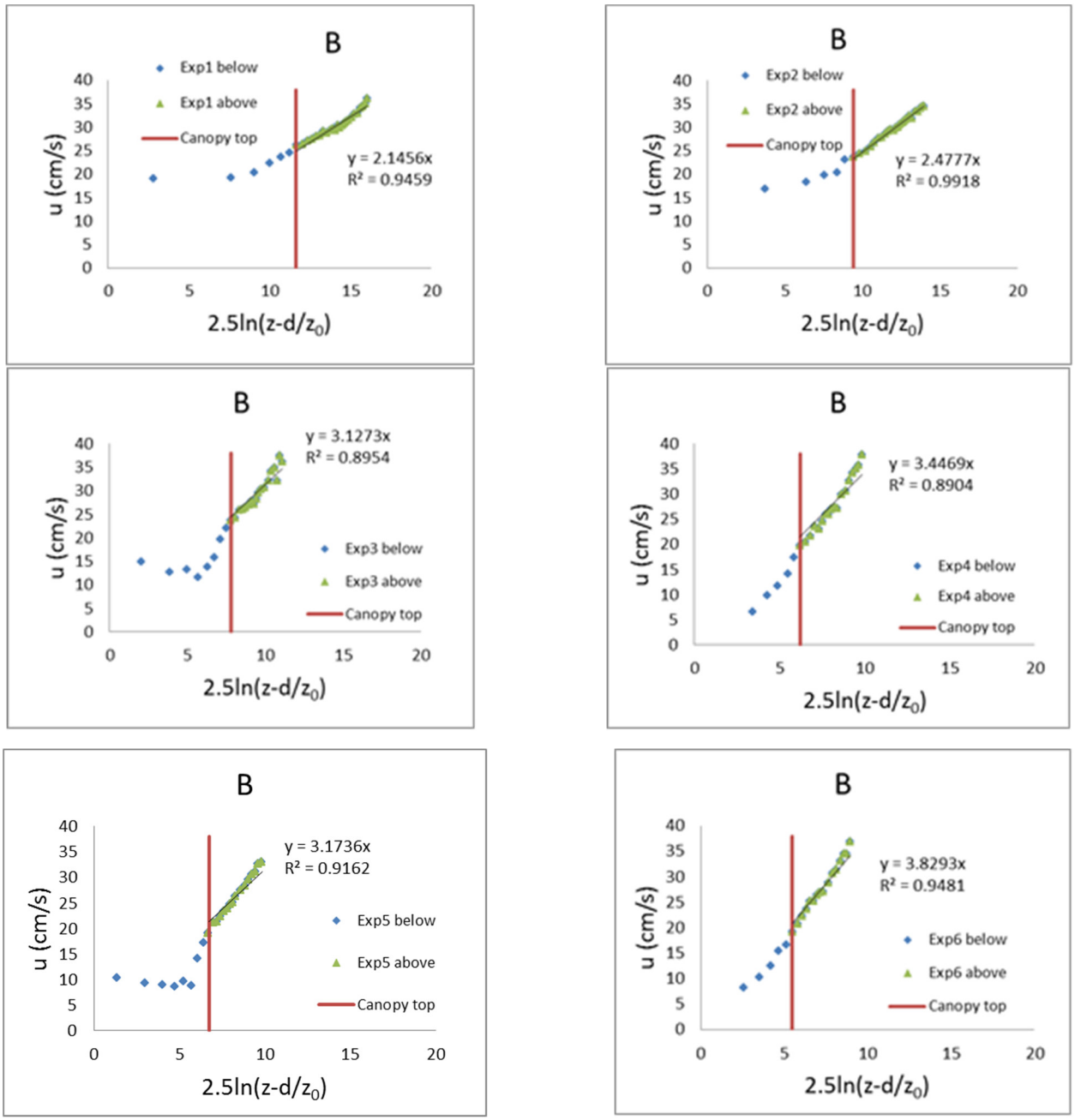

Figure 5. Fitting of Equation (1) to the present data above the canopy top at position B for all experiments following Raupach's [19] approach.

The values of u* for all experiments and positions, as well as those of d and z_0, are listed in Table 2. One may notice that: (a) for any given position, the values of u* are considerably larger for the compound elements compared to the simple rods as well as for the staggered (denser) pattern compared to the parallel one; (b) the values of u* for the two

types of compound elements are about the same for the sparse (parallel) placement pattern, although the frontal density λ is appreciably different; (c) the values of d and z_0 are also larger for the compound elements, but they differ appreciably between the two types of compound elements; and (d) for a given experiment, three groups of nearly identical u* values at positions along lines parallel to the elements' alignment may be identified, i.e., at (A,B,C), (D,E,F) and (G,H,I), suggesting a lateral differentiation of shear offered by the canopy to the upper non-vegetated layer.

Table 2. Main parameters of Raupach's and Nepf's models for the present experiments.

	Raupach [19]											**Nepf [9]**		
			u* (cm/s)											
	d (cm)	**z_0 (cm)**	**A**	**B**	**C**	**D**	**E**	**F**	**G**	**H**	**I**	**d (cm)**	**z_0 (cm)**	**u* (cm/s)**
Exp1	0.92	0.029	2.19	2.15	2.16	2.39	2.42	2.37	2.49	2.40	2.48	0	0.08	4.54
Exp2	1.22	0.065	2.47	2.48	2.47	2.56	2.59	2.51	2.77		2.71	0	0.16	4.54
Exp3	2.63	0.194		3.13		3.30	3.33	3.34	3.61	3.61	3.61	0	0.50	4.20
Exp4	3.32	0.306		3.45		3.52	3.59	3.53	3.80		3.80	1.58	1.97	4.20
Exp5	3.50	0.305		3.17		3.34	3.33	3.33	3.61	3.65	3.64	0.07	2.88	4.08
Exp6	4.32	0.411		3.83		4.04	4.07	4.09	4.45		4.48	4.06	1.44	4.08

Nepf [9], in a review of relevant previous work, considered the application of Equation (1) for aquatic canopies and proposed the following equations for evaluating the main parameters u*, d and z_0:

$$u^* = [gS(H - h)]^{0.5} \quad (5)$$

$$d/h = 1 - (0.1/C_D\lambda) \quad (6)$$

$$z_0/h \approx C_D\lambda; \text{ for } \lambda < 0.1 \quad (7a)$$

$$z_0/h = (0.04 \pm 0.02)\lambda^{-1}; \text{ for } \lambda > 0.1 \quad (7b)$$

where g is the acceleration of gravity, S is the sum of the slopes of the bottom and the free surface and C_D is a drag coefficient of order 1. Clearly, Equation (6) is valid for $\lambda > 0.1$, whereas d vanishes for $\lambda \leq 0.1$; consequently, Nepf [9] noted that, for a low vegetation density ($\lambda < 0.1$), there is no inflection point in the velocity profile, which tends to follow the same logarithmic law within and above the vegetation. Based on Equations (5)–(7), the values of d, z_0 and u* were computed for each experiment and are also listed in Table 2. Comparing these values with those obtained from Raupach's model, significant differences are observed. In particular, the u* values from Equation (5) are considerably larger than those of Raupach for the experiments with simple stems. They decrease slightly for the compound elements, and they are independent of the pattern/density for a given type of element. This behavior is due to the estimation of u* based solely on the depth (H-h) of the upper non-vegetated layer, without taking into account the fact that, in the present experiments, the flow depth H is artificially controlled instead of being naturally established by the flow through the canopy. It should be noted that a more accurate estimate based on the depth (H-d) [11] would produce only a marginal difference or no difference in the present case. The variation of the ratio of $\langle u^*_R \rangle / u^*_N$, where $\langle u^*_R \rangle$ denotes the average value of all positions for a given experiment according to Raupach's model and u^*_N denotes the value obtained from Nepf's model (i.e., Equation (5)), with the frontal density index λ, is plotted in Figure 6. A good correlation can be noticed, with a gradual increase in the shear velocity ratio with increasing λ in the range studied.

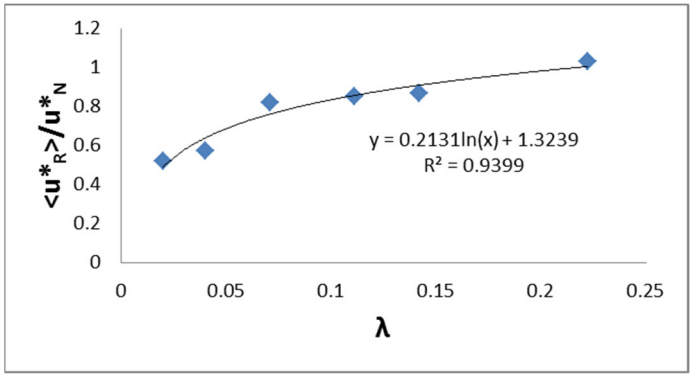

Figure 6. Variation of $\langle u^*_R \rangle / u^*_N$ with λ.

3.3. Velocity Distribution within and above the Vegetation

As mentioned in the Introduction, many efforts have been made to establish analytical expressions of the velocity distribution either in separate layers, e.g., as in [5,6,13,14], or over the entire water column, e.g., as in [9,12]. In principle, the velocity profile within the vegetation layer is expected to depend on the type of vegetation. In particular, for vertically non-uniform vegetation elements, it has been noted that the profile contains a part resembling a left round bracket "(", with a minimum at the level of the maximum frontal width [15]. Nevertheless, in the present study, the application of a unified distribution was attempted in order to reveal the extent of the influence of the element geometry in different positions within the vegetation. A relatively simple model, presented by Carollo et al. [12], was chosen, in which the following form of distribution is proposed:

$$u/u^* = b_0 + b_1 \arctan((Y-\alpha_1)/\alpha_2) \quad (8)$$

where $Y = z/h$, $\alpha_1 = h/H$. The profile of Equation (8) assumes an inflection point which was found to coincide with the top of the canopy; therefore, the constant $b_0 = u_h/u^*$. The coefficients α_2 and b_1 relate to the steepness of the distribution and to its width between maximum and minimum velocities near the free surface and the channel bottom, respectively. The model was implemented in the present case by determining the values of the constants, based on the measured velocities at the element top and at the maximum and minimum height z.

The results of the comparison of the measured velocity distribution with Equation (8) at certain measurement positions for Exp3 (B, E, F and H) are shown in Figure 7. The data points are marked differently for the lower (stem), intermediate (foliage) and upper (above canopy) layer. In the same figure, the logarithmic profile obtained previously following Raupach [19] is also shown. It may be seen that Equation (8) fits the data very well over the entire water column at positions E and H, in which there is gradual decrease in velocity towards the bottom; however, it is unable to describe the velocity distribution within the vegetation at positions B and F, in which the minimum velocity occurs in the intermediate foliage layer. It can also be observed that the logarithmic profile (Equation (1)) obtained for the upper layer satisfactorily describes the actual velocity also in the foliage layer at all positions.

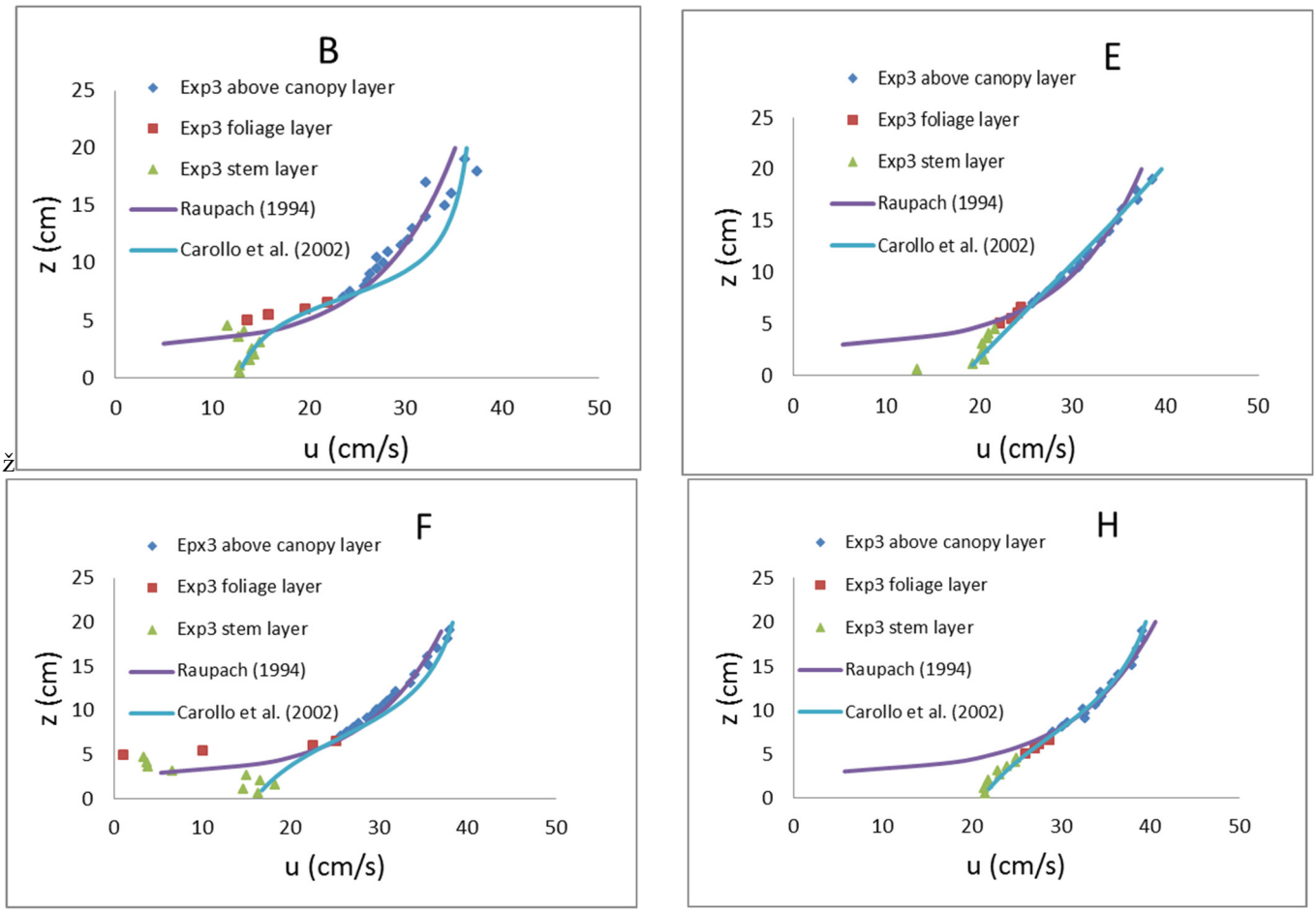

Figure 7. Velocity distribution data for Exp3, compared to equations of Raupach [19] and Carollo et al. [12].

The respective results at positions B and F for Exp1, Exp4 and Exp5 are presented in Figure 8, so as to illustrate the differences due to the type of element and the density of vegetation. It can be observed that, for the denser pattern (Exp4), as well for the compound rigid elements (Exp5), the fitting of Equation (8) is rather poor at B and F, similarly to Exp3. However, in the case of simple stems without foliage (Exp1), Equation (8) fits the data reasonably well over the entire water column at position B and even better at F, contrary to Exp3. This is clearly due to the absence of a locally minimum velocity at an intermediate level in the vegetated layer. Moreover, in Exp1, the logarithmic profile extends nearly to the bottom at B but not at F.

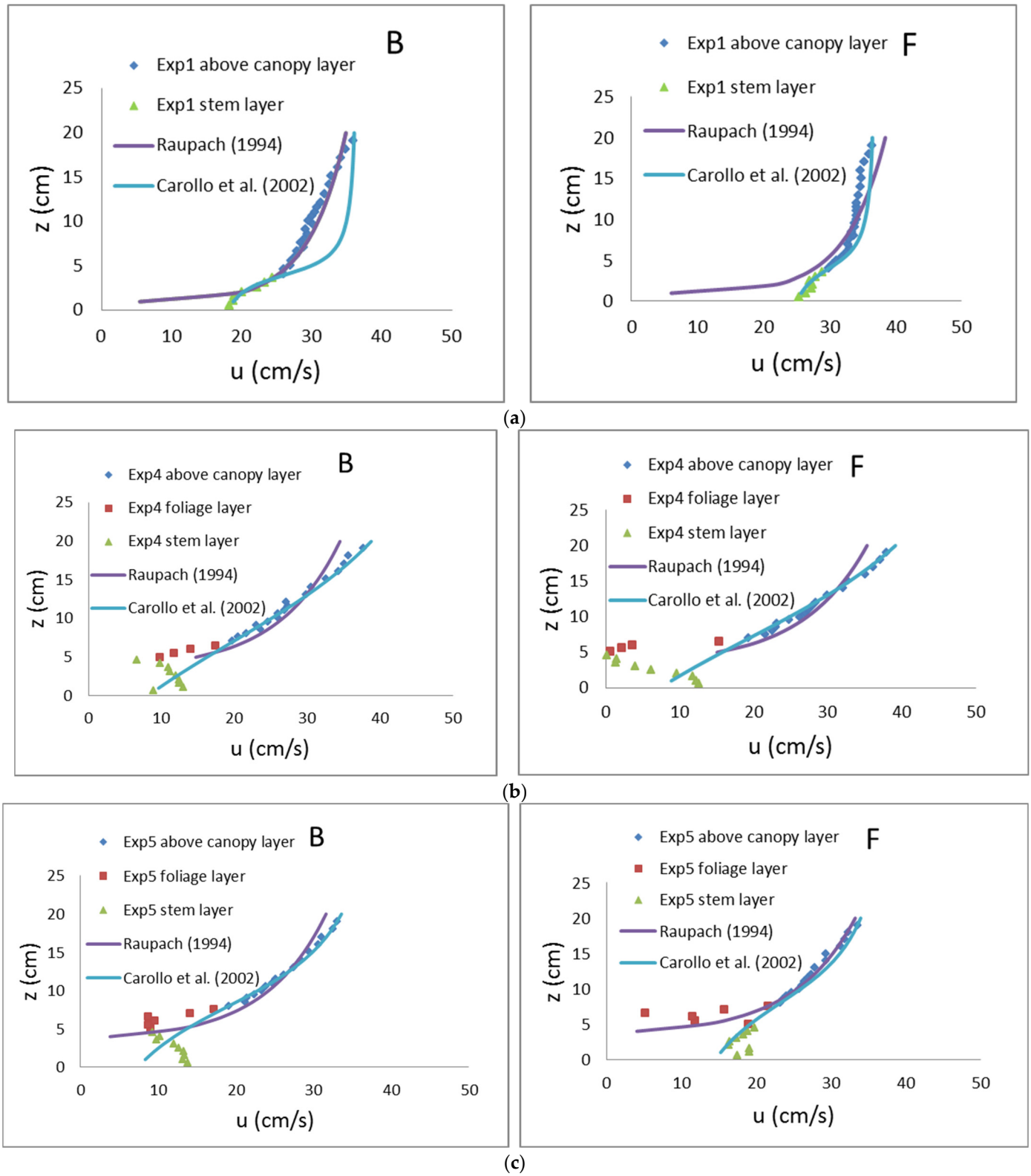

Figure 8. Velocity distribution data at B and F compared to equations of Raupach [19] and Carollo et al. [12] for (**a**) Exp1, (**b**) Exp4 and (**c**) Exp5.

4. Conclusions

A comprehensive experimental study was conducted with three different types of vegetation elements for evaluating the effects of element geometry and density on velocity

distributions in channels with submerged vegetation. From the results obtained, the following main conclusions may be drawn:

1. The logarithmic distribution originally developed by Raupach [19] for flow over terrestrial canopies is capable of well describing the velocity profile in the layer above the aquatic vegetation, with proper determination of its parameters. These were found to depend on the type and density of vegetation elements and also on the relative location with respect to the elements' alignment.
2. For vegetation without foliage, i.e., simple stems, the velocity generally decreases gradually towards the bottom, except at locations in close proximity to the elements where an abrupt decrease occurs. Thus, excluding those locations, a unified velocity distribution, such as the one proposed by Carollo et al. [12], provides good fit with the measurements over the entire water column.
3. For vegetation with foliage, the velocity distribution below the top of the canopy depends strongly on the relative location in the vegetation array and to a lesser extent on the pattern/density. At several locations, the distribution exhibits a minimum value at the level of the foliage, with the velocity reduction being more severe in between the elements' alignment.
4. The type of foliage of similar size, i.e., dense/rigid or sparse/flexible, appears to be of secondary importance concerning main features of the velocity distribution, such as the maximum velocity defect at the foliage level and the shear velocity offered to the upper free layer.

The present conclusions are, in principle, limited by the idealized form of the elements used. Natural vegetation with more complex geometry and randomness of patterns is likely to introduce additional variability for the flow conditions.

Author Contributions: Conceptualization, A.M. and G.C.; methodology, G.C.; experiments, A.M.; software, A.M.; validation, A.M. and G.C.; formal analysis, A.M.; investigation, A.M.; resources, G.C.; data curation, A.M.; writing—original draft preparation, A.M. and G.C.; writing—review and editing, G.C.; visualization, A.M.; supervision, G.C.; project administration, G.C.; funding acquisition, G.C. All authors have read and agreed to the published version of the manuscript.

Funding: This research received no external funding. The experimental work was partly supported by the NTUA Research Committee through the project "Research on problems of open channel flow and hydraulic structures".

Institutional Review Board Statement: Not applicable.

Informed Consent Statement: Not applicable.

Data Availability Statement: Detailed data may be obtained upon request from the first author (arismaur@central.ntua.gr).

Acknowledgments: Technical support for the experiments was provided by Ioannis Patselis.

Conflicts of Interest: The authors declare no conflict of interest. The funders had no role in the design of the study; in the collection, analyses or interpretation of data; in the writing of the manuscript; or in the decision to publish the results.

References

1. Kouwen, N.; Unny, T.E.; Hill, H.M. Flow retardance in vegetated channels. *J. Irrig. Drain. Div.* **1969**, *95*, 329–343. [CrossRef]
2. Stone, B.M.; Shen, H.T. Hydraulic resistance of flow in channels with cylindrical roughness. *J. Hydraul. Eng.* **2002**, *128*, 500–506. [CrossRef]
3. Jarvela, J. Flow resistance of flexible and stiff vegetation: A flume study with natural plants. *J. Hydrol.* **2002**, *269*, 44–54. [CrossRef]
4. Klopstra, D.; Barneveld, H.J.; van Noortwijk, J.M.; van Velzen, E.H. Analytical model for hydraulic roughness of submerged vegetation. In Proceedings of the 27th Congress of the International Association for Hydraulic Research, Theme A, Managing Water: Coping with Scarcity and Abundanc, San Francisco, CA, USA, 10–15 August 1997; pp. 775–780.
5. Huthoff, F.; Augustijn, D.C.M.; Hulscher, S.J.M.H. Analytical solution of the depth-averaged flow velocity in case of submerged rigid cylindrical vegetation. *Water Resour. Res.* **2007**, *43*, W06413. [CrossRef]

6. Righetti, M.; Armanini, A. Flow resistance in open channel flows with sparsely distributed bushes. *J. Hydrol.* **2002**, *269*, 55–64. [CrossRef]
7. Huai, W.X.; Wang, W.; Zeng, Y.H. Two-layer model for open channel flow with submerged flexible vegetation. *J. Hydraul. Res.* **2013**, *51*, 708–718. [CrossRef]
8. Shi, Z.; Hughes, J.M.R. Laboratory flume studies of microflow environments of aquatic plants. *Hydrol. Process.* **2002**, *16*, 3279–3289. [CrossRef]
9. Nepf, H.M. Flow and transport in regions with aquatic vegetation. *Annu. Rev. Fluid Mech.* **2012**, *44*, 123–142. [CrossRef]
10. Ghisalberti, M.; Nepf, H.M. Mixing layers and coherent structures in vegetated aquatic flows. *J. Geophys. Res.* **2002**, *107*, 3-1–3-11. [CrossRef]
11. Nepf, H.M.; Vivoni, E.R. Flow structure in depth-limited, vegetated flow. *J. Geophys. Res.* **2000**, *105*, 28547–28557.
12. Carollo, F.G.; Ferro, V.; Termini, D. Flow velocity measurements in vegetated channels. *J. Hydraul. Eng.* **2002**, *128*, 664–673. [CrossRef]
13. Huai, W.X.; Zeng, Y.H.; Xu, Z.G.; Yang, Z.H. Three-layer model for vertical velocity distribution in open channel flow with submerged rigid vegetation. *Adv. Wat. Res.* **2009**, *32*, 487–492. [CrossRef]
14. Chen, S.C.; Kuo, Y.M.; Li, Y.H. Flow characteristics within different configurations of submerged flexible vegetation. *J. Hydrol.* **2011**, *398*, 124–134. [CrossRef]
15. Li, Y.; Wang, Y.; Anim, D.O.; Tang, C.; Du, W.; Ni, L.; Yu, Z.; Acharya, K. Flow characteristics in different densities of submerged flexible vegetation from an open-channel flume study of artificial plants. *Geomorphology* **2014**, *204*, 314–324. [CrossRef]
16. Stephan, U.; Gutknecht, D. Hydraulic resistance of submerged flexible vegetation. *J. Hydrol.* **2002**, *269*, 27–43. [CrossRef]
17. Liu, D.; Diplas, P.; Fairbamks, J.D.; Hodges, C.C. An experimental study of flow through rigid vegetation. *J. Geophys. Res.* **2008**, *113*, F04015. [CrossRef]
18. Raupach, M.R. Drag and drag partition on rough surfaces. *Bound.-Layer Meteorol.* **1992**, *60*, 375–395. [CrossRef]
19. Raupach, M.R. Simplified expressions for vegetation roughness length and zero-plane displacement as functions of canopy height and area index. *Bound.-Layer Meteorol.* **1994**, *71*, 211–216. [CrossRef]
20. Fairbanks, J.D. Velocity and Turbulence Characteristics in Flows through Rigid Vegetation. Master's Dissertation, Virginia Polytechnic Institute & State University, Blacksburg, VA, USA, 1998.
21. Dunn, C.; Lopez, F.; Garcia, M.H. *Mean Flow and Turbulence in a Laboratory Channel with Simulated Vegetation*; Hydraulic Engineering Series 51; University of Illinois: Urbana, IL, USA, 1996.
22. Mavrommatis, A.; Christodoulou, G. Comparative experimental study of flow through various types of simulated vegetation. *Environ. Proc.* **2022**, *9*, 33. [CrossRef]